Synthesis and Corrosion Inhibition of Mild Steel in a Phosphoric Acid Solution of a Novel Benzothiazine Derivative

A. El khlifi[1], M. Saadouni[2], R. Ijoub[1], A. Oubihi[1], Y. Elaoufir[3], S. Boukhriss[2] and M. Ouhssine[1, *]

[1]Laboratory of Biotechnology, Environment and Quality, Faculty of Sciences, Ibn Tofaïl University, 14000 Kenitra, Morocco
[2] Laboratory of Organic, Organometallic and Theoretical Chemistry, Faculty of Science, Ibn Tofaïl University,14000 Kenitra, Morocco
[3] Laboratory of Organic Chemistry, Catalysis and Environment, Higher School of Education and Training, Ibn Tofaïl University, PB 133-14050, Kenitra, Morocco

[*]Corresponding author: ouhssineunivit@gmail.com

Received 02/03/2019; accepted 25/05/2021
https://doi.org/10.4152/pea.2022400103

Abstract
Ethyl 3-hydroxy-2-(p-tolyl)-3,4-dihydro-2H-benzo[b][1,4]thiazine-3-carboxylate (EHBT) inhibition effect and its adsorption onto a mild steel surface in phosphoric acid (2 M H_3PO_4) was investigated, at temperatures varying between 298 and 328 K, by weight loss, EIS and potentiodynamic polarization techniques. The tested compound showed an inhibition efficiency that was superior to 88 % for a concentration equal to 5×10^{-3} M. Polarization measurements indicated that the examined EHBT acted as a mixed inhibitor. The protection efficiency increased with higher inhibitor concentrations and decreased with an increase in temperature. EHBT adsorption onto the mild steel surface obeyed Langmuir adsorption isotherm. EHBT inhibition action was also evaluated by surface SEM images.

***Keywords**:* corrosion inhibition; benzothiazine; phosphoric acid; mild steel; and EIS.

Introduction

Phosphoric acid (H_3PO_4) is a medium-strong acid, but it still shows strong corrosiveness on ferrous and ferrous alloys (1); it is widely used in the production of fertilizers and steel surface treatment, such as chemical and electrolytic polishing or etching, chemical coloring, oxide film removal, phosphating, passivating and surface cleaning. There is a great need to protect steel materials used in the phosphoric acid industry. Up to now, little work (2, 3) appears to have been done on steel corrosion inhibition in H_3PO_4 solutions.

Considerable efforts are being made to find suitable compounds to be used as corrosion inhibitors in various corrosive media (4-12). One way to protect metal surfaces from oxidative corrosion is the use of the so-called corrosion inhibitors. Small amounts of these compounds are dissolved in corrosive media to protect the metal surface. To date, a large variety of different inhibitors has been studied in several corrosive media and on various metal surfaces (13-16).

Interestingly, there is a great interest in 1.4-benzothiazines which are increasingly being investigated for applications in the growing field of medicine. In fact, the 1,4-benzothiazines are the best known to possess biologically diverse activities (17) such as antimicrobial (18) antifungal (19) antioxidant agents (20) and anticancer (21, 22). Compounds based on the 1,4-benzothiazine moiety offer a high degree of structural diversity and have proven to be broadly and economically useful as therapeutics (23-25). It is the core structure in many drugs and biologically active natural products (26, 27). Sulfur-containing corrosion inhibitors have greatly interesting molecular structures compared with other classes of compounds. Their high protective effect for steels is due to the presence of the S atom in molecular structures (28). It is widely reported that highly efficient heteroatoms such as oxygen, nitrogen, phosphorus and sulfur follow the sequence of O < N < S < P, which makes sulfur-containing compounds excellent inhibitors (29, 30).

In the present work, mild steel (MS) corrosion inhibition effect in 2.0 M H_3PO_4 by Ethyl 3-hydroxy-2-(p-tolyl)-3,4-dihydro-2H-benzo[b][1,4]thiazine-3-carboxylate (EHBT) was investigated using weight loss, potentiodynamic polarization methods, electrochemical impedance spectroscopy (EIS) and scanning electron microscopy (SEM).

Experimental details

Synthesis

The general procedure for the preparation of two 1,4-benzothiazines derivatives was a solution of epoxide 1 (1 mmol) in acetonitrile (20 mL) added to 2-aminothiophenol (1 mmol). The mixture was refluxed for 25 h. The hydrogen cyanide was trapped by a 0.1 M KOH solution in a bubbler. Then, the solvent was removed under a reduced pressure, and the obtained residue was purified by flash chromatography on a silica column eluted with chloroform/ petroleum ether in the ratio of 2 : 1.

The result was Ethyl-3-hydroxy-2-(p-tolyl)-3,4-dihydro-2H-benzo[b][1,4]thiazine-3-carboxylate (EHBT): 0,19 g (60%). Infrared Spectroscopy (IR) for KBr (cm-1) gave the following results: 3378 (NH), 2982 (OH), 1746 (CO). The signals of diastereomer 1 were: 1H NMR (300 MHz, DMSO-d6): _ 2.40 (s, 3H, CH3), 4.7 (s, 1H, CHS), 1.28 (t, 3H, CO2CH2CH3), 4.7 (q, 2H, CO2CH2CH3), 6.4-7.5 (m, Ar); 13C NMR (75 MHz, DMSO-d6): _ 14.21, 21.49, 57.0, 63.92, 83.92, 115.28, 116.56, 122.69, 125.80, 127.22, 128.01, 130.36, 134.81, 140.14, 150.21 and 162.77. The signals of diastereomer 2 were: 1H NMR (300 MHz, DMSO-d6): _ 2.30 (s, 3H, CH3), 4.7 (s, 1H, CHS), 1.21 (t, 3H, CO2CH2CH3), 4.29 (q, 2H, CO2CH2CH3), 6.4-7.5 (m, Ar); 13C NMR (75 MHz, DMSOd6): _14.31, 21.34, 57.0, 62.37, 83.92, 114.29, 117.01, 123.17, 127.01, 127.59, 129.55, 130.75, 135.90, 141.92, 154.08 and 167.0. Electron Ionization Mass Spectroscopy (EIMS) results were: m/z (C18H19NO3S) 225 (100%), 116 (7.14%), 91 (7.14%) and 108 (17.14%).

Electrodes, chemicals and test solution

Corrosion tests have been performed, using gravimetric and electrochemical measurements, on electrodes cut from carbon steel sheets with the chemical

composition: 0.370 % C, 0.230 % Si, 0.680 % Mn, 0.016 % S, 0.077 % Cr, 0.011 % Ti, 0.059 % Ni, 0.009 % Co, 0.160 % Cu and the remainder iron. The phosphoric acid aggressive media used for all studies were prepared by the dilution of analytical grade 85% H_3PO_4 with double distilled water. EHBT concentrations used in this investigation were varied from 10^{-4} to 5×10^{-3} M.

Gravimetric measurements

Gravimetric measurements were realized in a double walled glass cell equipped with a thermostat-cooling condenser. The used mild steel specimens with a rectangular form of the dimensions 2.5 × 2.0 × 0.2 cm^3 were abraded with different grades of emery paper (320, 800 and 1200), and then washed thoroughly with distilled water and acetone. After accurately weighing, the specimens were immersed in beakers which contained 100 mL acid solutions, without and with various EHBT concentrations**,** at a temperature equal to 303 K, and remained immersed in a water thermostat for 6h. The gravimetric tests were performed by triplicate at the same conditions. The mild steel corrosion rates (C_R) and inhibition efficiency (η_w %) have been evaluated from mass loss measurements using the following equations:

$$\eta_w = \frac{C_R - C'_R}{C_R} \times 100 \quad (1)$$

$$\theta = 1 - \frac{C'_R}{C_R} \Rightarrow \theta = \frac{(\eta_w\%)}{100} \quad (2)$$

where C_R and C'_R are the mild steel corrosion rates in phosphoric acid, without and with the studied range of EHBT concentrations, respectively, and θ is the degree of surface coverage.

Electrochemical measurements

Electrochemical measurements, including stationary (PDP) and transient (EIS) methods were performed in a three-electrode cell. A pure mild steel specimen as working electrode, a saturated calomel (SCE) as reference electrode and an area platinum as counter electrode (CE) were used. All potentials were measured against SCE. The working electrode was immersed in a test solution for 30 min, until the corrosion potential of the equilibrium state (E_{corr}) was achieved, using a type PGZ100 potentiostat. From Fig. 1, we can observe that there is no substantial variation in the open circuit potential for the last 15 min, confirming that the steady state was reached.

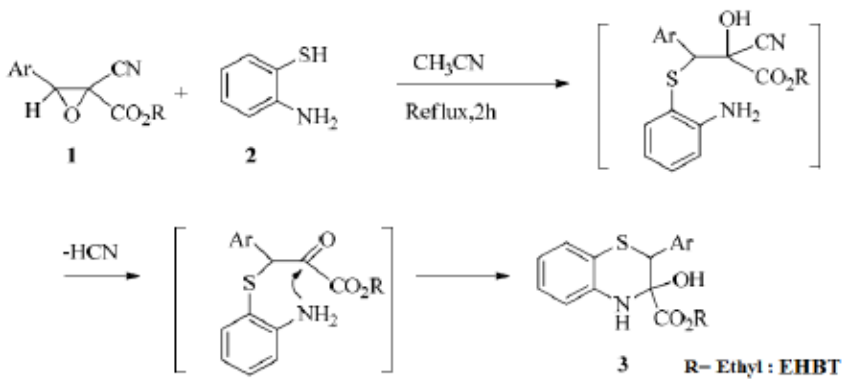

Figure 1. Synthesis of 1,4-benzothiazines derivative.

The potentiodynamic polarization curves were determined by a constant sweep rate of 1 mv/s. The transitory method (EIS) measurements were determined using ac amplitude signals of 10 mV peak to peak, at different conditions, in the frequency range from 100 kHz to 10 mHz. The data obtained by the EIS method were analyzed and fitted using graphing and analyzing impedance software, version Zview2. For the potentiodynamic polarization (PDP) method, the inhibition efficiency of the studied compound was calculated using the following equation:

$$\eta_{PDP}(\%) = \left[1 - \frac{i_{corr}}{i^{\circ}_{corr}}\right] \times 100 \qquad (3)$$

where i_{corr} and i°_{corr} are the corrosion rates in the inhibitor presence and absence, respectively. The impedance diagrams were determined by the EIS method. To confirm reproductibility, all experiments were repeated three times, and the evaluated inaccuracy did not exceed 10%. For the EIS method, the inhibition efficiency was calculated using the following equation:

$$\eta_{EIS}(\%) = \left[\frac{R_{p(inh)} - R_p}{R_{p(inh)}}\right] \times 100 \qquad (4)$$

where R_p and $R_{p\ (inh)}$ are the mild steel electrode polarisation resistance in the uninhibited and inhibited solutions, respectively.

In Fig. 2, OCP vs. time curves for mild steel in 2 M H_3PO_4, with the absence and presence of different EHBT concentrations, at 298 K, were recorded.

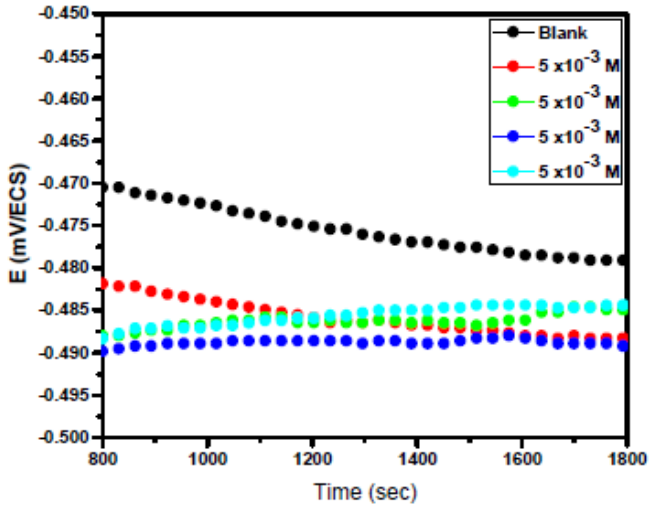

Figure 2. OCP vs. time curves for mild steel in a 2 M H_3PO_4 solution, in the presence and absence of different EHBT concentrations, at 298 K.

SEM

The changes in the mild steel surface morphology, in the absence and presence of the optimum EHBT concentration, were studied using Scanning Electron Microscopy (SEM), after 6h of immersion, at 303 K. SEM (Hitachi TM-1000), with an accelerating voltage of 15 kV, was used for the experiments.

Results and discussion

Polarization results

In Fig. 3, the anodic and cathodic plots were recorded on the mild steel electrode in 2 M H_3PO_4, with the absence and presence of different EHBT concentrations, at

298 K. The associated electrochemical parameters, such as corrosion potential (E_{corr}), corrosion current density (i_{corr}), anodic and cathodic Tafel slopes (βa and βc), which were obtained from the intersection of anodic and cathodic Tafel lines, and the corrosion inhibition efficiencies, η_{PDP} ($^0/_0$), were calculated, and are shown in Table 1.

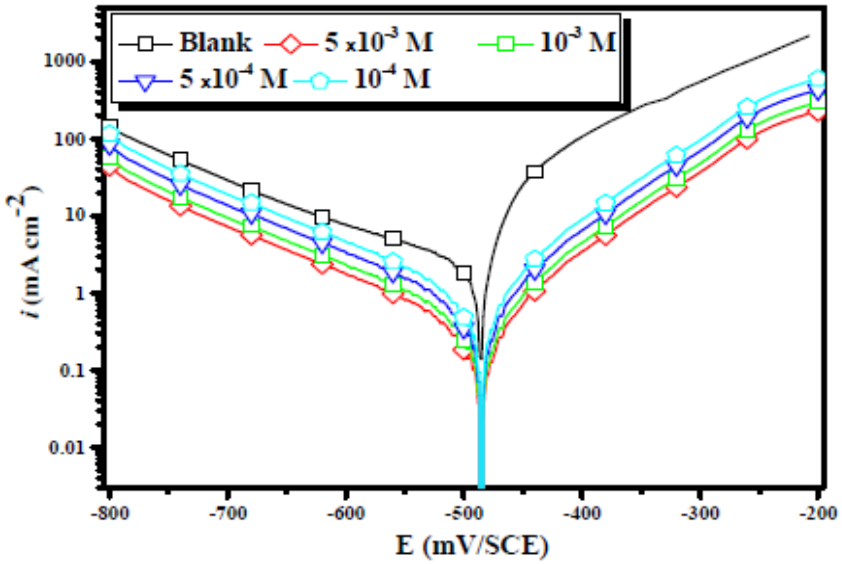

Figure 3. Potentiodynamic polarization curves for mild steel in a 2 M H_3PO_4 solution, in the presence and absence of different EHBT concentrations, at 298 K.

Table 1. Electrochemical parameters calculated by the PDP technique for mild steel corrosion in 2 M H_3PO_4, in the absence and presence of different EHBT concentrations, at 298 K.

Inhibitor	Concentration (g/L)	$-E_{corr}$ (mV/SCE)	$-\beta_c$ (mV/dec)	β_a (mV/dec)	i_{corr} (μA/cm²)	η_{PDP} ($^0/_0$)
H_3PO_4	2 M	488	135	92	2718	-
	5×10^{-3}	487	139	86	313	88
	1×10^{-3}	485	137	92	434	84
EHBT	5×10^{-4}	488	133	87	645	76
	1×10^{-4}	486	136	84	865	68

Moreover, all the cathodic curves were nearly parallel, suggesting that the cathodic reactions mechanism did not change in the inhibitor presence. This leads us to attribute the decreases in the cathodic current densities to the blockage of the cathodic sites caused by the EHBT molecules adsorpsion onto the mild steel surface, which has diminished the rates of both cathodic reactions. We have also concluded that the EHBT corrosion inhibition on mild steel was caused by a geometric blocking effect (31). Namely, the inhibition effect comes from the reduction of the reaction area on the corroding metal surface (31). βc and βa Tafel slopes did not change upon EHBT addition, which means that the inhibitor presence did not change the reaction mechanism. It can also be seen that both the anodic and cathodic currents were shifted to lower values, at the same potential, with higher inhibitor concentrations.

This behavior indicates that both the anodic and cathodic reactions were suppressed, i.e., EHBT is a mixed-type inhibitor (32, 33). In addition, it was

observed that the higher the C_{inh}, the higher the η_{PDP} ($^0/_0$), as a result of the increase in θ.

Electrochemical impedance spectroscopy (EIS)

Mild steel corrosive behavior, with and without the inhibitor in 2 M H_3PO_4, has been reported by employing EIS measurements, at 298 K. Nyquist plots on mild steel, in the absence and presence of various EHBT inhibitor concentrations in 2 M H_3PO_4, are given in Fig. 3. It was manifest that, with the EHBT addition to the H_3PO_4 aggressive solution, the mild steel impedance has significantly improved. The impedance plots for concentrations were found to be similar (Fig. 4).

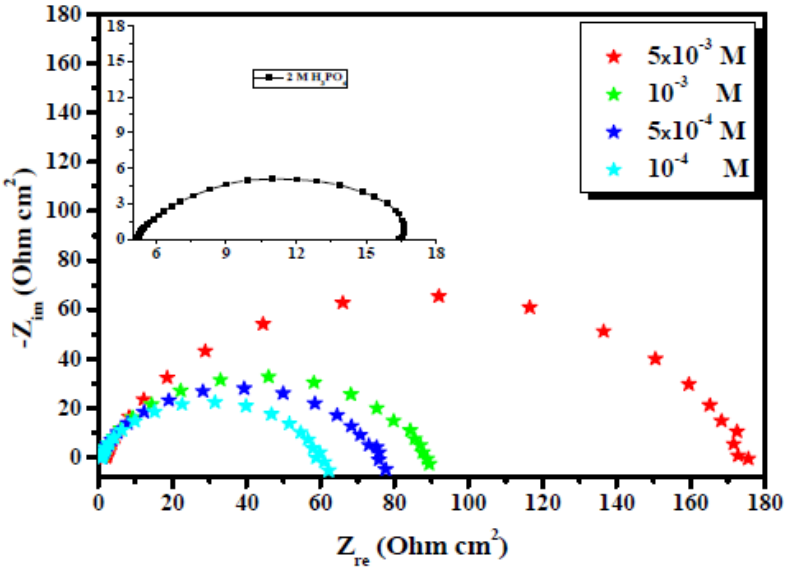

Figure 4. Nyquist plots for carbon steel in a 2 M H_3PO_4 solution containing various EHBT concentrations, at 298 K.

Equivalent circuits are usually used to analyze EIS data (34-36). For example, Fig. 5 shows a simple equivalent circuit with one-time constant that is commonly used to analyze the measured impedance of a uniformly corroding electrode in an electrolyte.

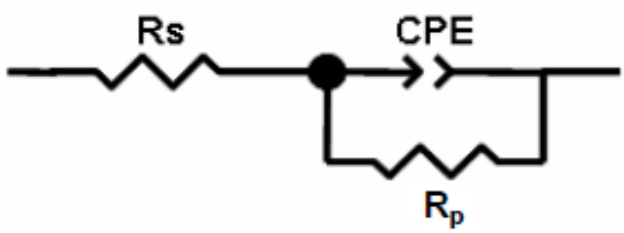

Figure 5. Equivalent electrical circuit.

This circuit consists of an electrolyte resistance (R_s), a polarization resistance (R_p) and a constant phase element (CPE), which is used for a non-ideal double layer. The non-ideal capacitance behavior of a double layer can be attributed to many factors, e.g., surface roughness and non-uniform surface coverage, corrosion rate

or current distribution (37, 38). The impedance of this element is frequency-dependent, and it can be calculated using the following equation:

$$Z_{CPE} = \frac{1}{Q(j\omega)^n} \quad (5)$$

where Q is the CPE constant (in Ω^{-1} S^n cm^{-2}), ω is the angular frequency (in rad s^{-1}), $j^2 = -1$ is the imaginary number and n is a CPE exponent which can be used as a gauge for the surface heterogeneity or roughness (39, 40). In addition, the double layer capacitances, C_{dl}, for a circuit including a CPE, were calculated by using the following equation:

$$C_{dl} = \sqrt[n]{Q \times R_p^{1-n}} \quad (6)$$

It can be clearly seen from Fig. 4 that the Nyquist plots show a single capacitive semicircle shape at higher frequencies in the inhibitor presence. This indicates that mild steel corrosion in a 2 M H_3PO_4 solution is mainly controlled by a charge transfer process (41-43). The direct relationship between the capacitive loop diameter and the EHBT inhibitor concentration can be attributed to the increase in the polarization resistance (R_{ct}), as a result of the increase in the corrosion inhibitor surface coverage (44). Consequently, the $\eta_{EIS}(\%)$ value is expected to increase with higher inhibitor concentrations, exactly as is found and shown in Table 2.

Table 2. Impedance parameters recorded for the mild steel electrode in a 2 M H_3PO_4 solution, in the absence and presence of different inhibitor concentrations, at 298 K.

Inhibitor	Concentration (M)	R_p (Ω cm^2)	Q×10^{-4} (s^n Ω^{-1}cm^{-2})	n	C_{dl} (μF/cm^2)	η_{EIS} (%)
H_3PO_4	2.0	14	2.1024	0.88	94.96	—
EHBT	5×10^{-3}	173	0.4531	0.86	20	92
	1×10^{-3}	86	0.6188	0.88	30	83
	5×10^{-4}	70	0.8344	0.87	38	80
	1×10^{-4}	59	1.0113	0.85	40	76

In Table 2, it is evident that the R_p values increase and that the capacitance values, C_{dl}, decrease with higher inhibitor concentrations. Decrease in C_{dl}, which can result from a reduction in the local dielectric constant and/or from an increase in the double layer thickness, suggests that the inhibitor molecules inhibit mild steel corrosion by an adsorption process at the metal-solution interface (45). It is well known that the capacitance is the reciprocal of the double layer thickness (46). A low capacitance value may also result in a larger replacement of water molecules by the inhibitor molecules, through the adsorption at the electrode surface (46). Also, larger molecules of the inhibitor may also reduce the capacitance through an increase in double layer capacitance. Moreover, the protective layer thickness that has increased with higher inhibitor concentrations results in a significant decrease in C_{dl}.

Weight loss study

The corrosion rate, inhibiting efficiencies and cover surface values obtained from the weight loss method, with different inhibitor concentrations, at 298 K, are given in Table 3.

Table 3. Effect of EHBT concentration on the mild steel corrosion data in 2.0 M H_3PO_4.

Inhibitor	Concentration (M)	C_R (mg cm^{-2} h^{-1})	η_w (%)	Θ
Blank	2.0	5.061	-	-
EHBT	5×10^{-3}	0.796	84	0.84
	1×10^{-3}	0.913	82	0.82
	5×10^{-4}	1.109	78	0.78
	1×10^{-4}	1.308	74	0.74

It is clear from this table that the EHBT addition to the corrosive solution led to a decrease in the mild steel corrosion rate. Consequently, the inhibition effect and the surface coverage increased with higher concentrations of the tested inhibitor. The explanation of this behavior can be justified by the strong interaction of the inhibitor molecules with the metal surface, which results in adsorption.

Adsorption isotherm

Because the adsorption isotherm provides some structural and thermodynamic information, it is of great importance in the corrosion field (47-49). Generally, the inhibitors adsorption is largely influenced by the nature of the testing media, the chemical structure, the charge distribution, and by the metal nature (50, 51). To find a suitable adsorption isotherm in the present study, several commonly used isotherms were tested, among which the Langmuir adsorption isotherm was found to fit well with our experimental data (Fig. 6). The Langmuir isotherm can be represented as (52):

$$\frac{C_{inh}}{\theta} = \frac{1}{K_{ads}} + C_{inh} \qquad (7)$$

where C_{inh} is the concentration and K_{ads} is the equilibrium constant of the adsorption process. K_{ads} is related to the standard free energy of adsorption, ΔG°_{ads}, by the following equation (52):

$$\Delta G^{\circ}_{ads} = -RT\, ln(K_{ads} \times 55.5) \qquad (8)$$

where R represents the gas constant and T is the absolute temperature. The value of 55.5 is the water concentration in the solution in mol/L.

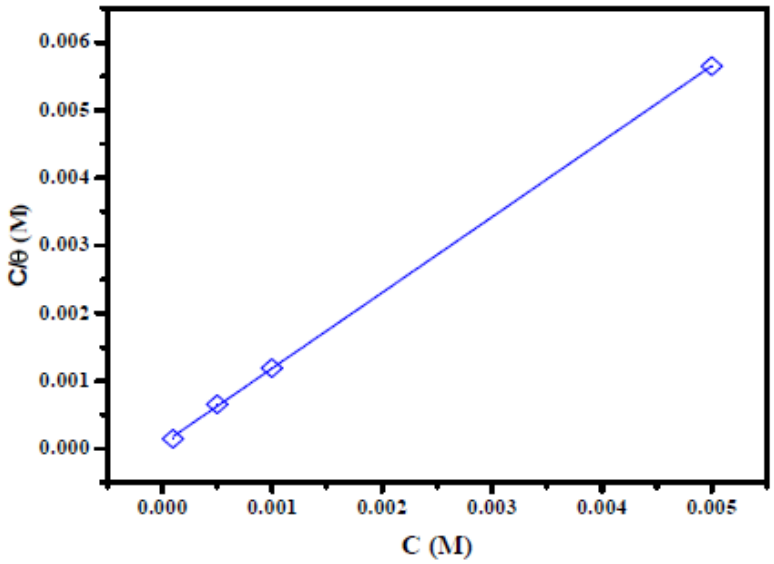

Figure 6. Langmuir adsorption of the inhibitor onto the mild steel surface in a 2 M H_3PO_4 solution, at 298K.

It has been mentioned in various literature that ΔG_{ads} values up to −20 kJ mol^{-1} are consistent with an electrostatic interaction between the charged inhibitor molecules and a charged metal (physical adsorption), while those nearly −40 kJ mol^{-1} or higher correspond to the charge sharing or charge transfer from the inhibitor molecules to the metal surface, to form a co-ordinate type of bond (chemical adsorption) (53,54). The calculated ΔG_{ads} value for the studied inhibitor is -38 kJ mol^{-1} (Table 4). This suggests a chemical and physical mode of adsorption.

Table 4. Adsorption parameters for carbon steel corrosion in 1.0 M HCl, at 303 K.

Inhibitor	Slope	K_{ads} (M^{-1})	R^2	ΔG_{ads} (kJ/mol)
EHBT	1.08	14933	0.999	- 38

Surface characterization

SEM images of the mild steel surface were taken to analyze the morphology before and after the inhibition process. The MS sample, in the inhibitor absence, shows a rough and highly damaged surface, due to the rapid corrosion attack of 2.0 M H_3PO_4, as shown in Fig. 7 (b), compared to an un-attacked steel (Fig. 7(a)), while Fig. 7(c) shows a smooth and less damaged mild steel surface, in the inhibitor presence. The protected surface obtained for mild steel in the inhibitor presence might be attributed to the inhibitor molecules adsorption.

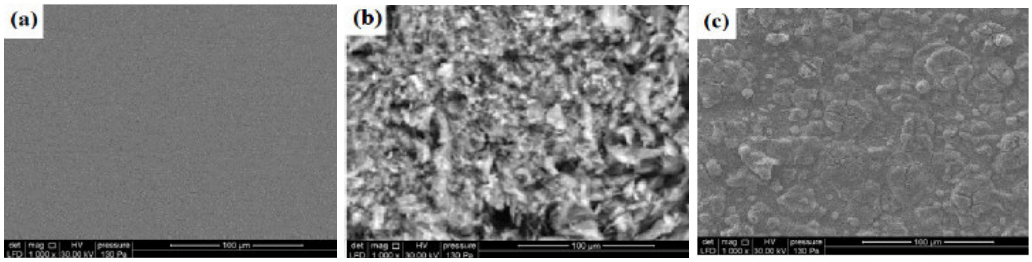

Figure 7. SEM micrographs in **(a)** polished steel and **(b)** in EHBT absence and **(c)** presence, at 5×10^{-3} M.

Conclusion

In the present work, a new benzothiazine derivative has been synthesized and then tested as a mild steel corrosion inhibitor in 2 M H_3PO_4. The tested compound (EHBT) acted as a good inhibitor for mild steel corrosion in a 2.0 M H_3PO_4 solution. Its inhibitive effect increased with higher concentrations, and slightly decreased at higher temperatures. EHBT acted as a mixed type inhibitor by blocking both cathodic and anodic corrosion reactions. EHBT adsorption onto the mild steel surface followed Langmuir adsorption isotherm. SEM images suggest that the inhibitor addition to aggressive solutions resulted in the formation of a protective film on the steel surface.

References

1. Bousskri A, Salghi R, Anejjar A, et al. The inhibition effect of 1-pentyl pyridazinium bromide towards copper corrosion in phosphoric acid containing

chloride. Port Electrochim Acta. 2016;34:1-21. https://doi.org/10.4152/pea.201601001
2. Belghiti ME, Nahlé A, Ansari A, et al. Inhibition effect of E and Z conformations of 2-pyridinealdazine on mild steel corrosion in phosphoric acid. Anti-Corros Methods Mater. 2017;64(1):23-35. https://doi.org/10.1108/ACMM-11-2015-1594
3. Uwineza MS, Essahli M, Lamiri A. Corrosion inhibition of aluminium in 2 M phosphoric acid using the essential oil of mentha pulegium leaves. Port Electrochim Acta. 2016;34(1):53-62. https://doi.org/10.4152/pea.201601053
4. Naciri M, El Aoufir Y, Lgaz H, et al. Exploring the potential of a new 1,2,4-triazole derivative for corrosion protection of carbon steel in HCl: A computational and experimental evaluation. Colloids Surf Physicochem Eng Asp. 2020 Jul 20;597:124604. https://doi.org/10.1016/j.colsurfa.2020.124604.
5. Khamaysa OMA, Selatnia I, Zeghache H, et al. Enhanced corrosion inhibition of carbon steel in HCl solution by a newly synthesized hydrazone derivative: Mechanism exploration from electrochemical, XPS, and computational studies. J Mol Liq. 2020;315:113805. https://doi.org/10.1016/j.molliq.2020.113805
6. El Aoufir Y, Zehra S, Lgaz H, et al. Evaluation of inhibitive and adsorption behavior of thiazole-4-carboxylates on mild steel corrosion in HCl. Colloids Surf Physicochem Eng Asp. 2020;606:125351. https://doi.org/10.1016/j.colsurfa.2020.125351
7. Singh A, Ansari KR, Quraishi MA, et al. Effect of Electron Donating Functional Groups on Corrosion Inhibition of J55 Steel in a Sweet Corrosive Environment: Experimental, Density Functional Theory, and Molecular Dynamic Simulation. Materials. 2019 ;12(1):17. https://doi.org/10.3390/ma12010017
8. Singh A, Ansari KR, Quraishi MA, et al. Synthesis and investigation of pyran derivatives as acidizing corrosion inhibitors for N80 steel in hydrochloric acid: Theoretical and experimental approaches. J Alloys Compd. 2018;762:347-62. https://doi.org/10.1016/j.jallcom.2018.05.236
9. Pareek S, Jain D, Hussain S, et al. A new insight into corrosion inhibition mechanism of copper in aerated 3.5 wt.% NaCl solution by eco-friendly Imidazopyrimidine Dye: experimental and theoretical approach. Chem Eng J. 2019;358:725-42. https://doi.org/10.1016/j.cej.2018.08.079
10. Saini N, Kumar R, Lgaz H, et al. Minified dose of urispas drug as better corrosion constraint for soft steel in sulphuric acid solution. J Mol Liq. 2018;269:371-80. https://doi.org/10.1016/j.molliq.2018.08.070
11. Kr. Saha S, Banerjee P. Introduction of newly synthesized Schiff base molecules as efficient corrosion inhibitors for mild steel in 1 M HCl medium: an experimental, density functional theory and molecular dynamics simulation study. Mater Chem Front. 2018;2(9):1674-91.
12. Kr. Saha S, Dutta A, Ghosh P, et al. Novel Schiff-base molecules as efficient corrosion inhibitors for mild steel surface in 1 M HCl medium: experimental and theoretical approach. Phys Chem Chem Phys. 2016;18(27):17898-911. https://doi.org/10.1039/C6CP00827E

13. Chaouiki A, Lgaz H, Zehra S, et al. Exploring deep insights into the interaction mechanism of a quinazoline derivative with mild steel in HCl: electrochemical, DFT, and molecular dynamic simulation studies. J Adhes Sci Technol. 2019;33(9):921-44. https://doi.org/10.1080/01694243.2018.1554764
14 Chaouiki A, Lgaz H, Salghi R, et al. Inhibitory effect of a new isoniazid derivative as an effective inhibitor for mild steel corrosion in 1.0 M HCl: combined experimental and computational study. Res Chem Intermed. 2020;46(6):2919-50. https://doi.org/10.1007/s11164-020-04119-6
15. Chafiq M, Chaouiki A, Lgaz H, et al. New spirocyclopropane derivatives: synthesis and evaluation of their performances toward corrosion inhibition of mild steel in acidic media. Res Chem Intermed. 2020;46(6):2881-918. https://doi.org/10.1007/s11164-020-04108-98
16. Lgaz H, Zehra S, Albayati MR, et al. Corrosion inhibition of mild steel in 1.0 M HCl by two hydrazone derivatives. Int J Electrochem Sci. 2019;14(7):6667-81. https://doi.org/10.20964/2019.07.08
17. Deshmukh M, Deshmukh S, Jagtap S, et al. Synthesis and study of biological activity of some new 1, 4-benzothiazines. Ind J Chem. 2007;46B:852-859.
18. Armenise D, Trapani G, Arrivo V, et al. Research on potentially bioactive aza and thiaza polycyclic compounds containing a bridgehead nitrogen atom. III. Synthesis and antimicrobial activity of some 1, 4-benzothiazines and pyrrolobenzothiazines. J Heterocycl Chem. 2000;37(6):1611-6. https://doi.org/10.1002/jhet.5570370634
19. Armenise D, De Laurentis N, Rosato A, et al. Synthesis and antimicrobial activity of 2-(acyl or carboxyalkyl)-3-(H or alkyl or aryl)-5 (or-6 or-8)-monochloro, 7-fluoro-substituted-4H-1, 4-benzothiazines. J Heterocycl Chem. 2006;43(5):1371-8. https://doi.org/10.1002/jhet.5570430536
20. Kumar M, Sharma K, Samarth R, et al. Synthesis and antioxidant activity of quinolinobenzothiazinones. Eur J Med Chem. 2010;45(10):4467-72. https://doi.org/10.1016/j.ejmech.2010.07.006
21. Gupta R, Gupta V. Synthesis and Spectral studies of Nitrosourea derivatives of 3-Methyl-5/7-Substituted-2-(3, 4-dichloro) benzoyl-4H-1, 4-Benzothiazines as Bifunctional Anticancer Agents. Heterocycl Commun. 2010;16(1):65-71. https://doi.org/10.1515/HC.2010.16.1.65
22. Thomas L, Gupta A, Gupta V. Synthesis of 2-amino-5-chloro-3-(trifluoromethyl) benzenethiol and conversion into 4H-1, 4-benzothiazines and their sulfones. J Fluor Chem. 2003;122(2):207-13. https://doi.org/10.1016/S0022-1139(03)00092-7
23. Sonawane AE, Pawar YA, Nagle PS, et al. Synthesis of 1,4-Benzothiazine Compounds Containing Isatin Hydrazone Moiety as Antimicrobial Agent. Chin J Chem. 2009;27(10):2049-54. https://doi.org/10.1002/cjoc.200990344
24. Pawar Y, Sonawane A, Nagle P, et al. Synthesis of 1, 4-benzothiazine compound containing isatin moieties as antimicrobial agent. Int J Curr Pharm Res. 2011;3:47-51.
25. Sabatini S, Gosetto F, Serritella S, et al. Pyrazolo [4, 3-c][1, 2] benzothiazines 5, 5-dioxide: a promising new class of Staphylococcus aureus Nora efflux

pump inhibitors. J Med Chem. 2012;55(7):3568-3572. https://doi.org/10.1021/jm201446h
26. Hni B, Sebbar NK, Anouar EH, et al. Syntheses, crystal structures, spectroscopic characterizations, DFT calculations, hirshfeld surface analyses and monte carlo simulations of novel long-chain alkyl-substituted 1,4-benzothiazine derivatives. J Mol Struct. 2020;1221:128886. https://doi.org/10.1016/j.molstruc.2020.128886
27. Ellouz M, Sebbar NK, Fichtali I, et al. Synthesis and antibacterial activity of new 1, 2, 3-triazolylmethyl-2H-1, 4-benzothiazin-3 (4H)-one derivatives. Chem Cent J. 2018;12(1):123. https://doi.org/10.1186/s13065-018-0494-2
28. Tang J, Hu Y, Han Z, et al. Experimental and Theoretical Study on the Synergistic Inhibition Effect of Pyridine Derivatives and Sulfur-Containing Compounds on the Corrosion of Carbon Steel in CO2-Saturated 3.5 wt.% NaCl Solution. Molecules. 2018;23(12):3270. https://doi.org/10.3390/molecules23123270
29. Rahal HT, Abdel-Gaber AM, Younes GO. Inhibition of Steel Corrosion in Nitric Acid by Sulfur Containing Compounds. Chem Eng Commun. 2016;203(4):435-45. https://doi.org/10.1080/00986445.2015.1017636
30. Quraishi MA, Shukla SK. Poly(aniline-formaldehyde): A new and effective corrosion inhibitor for mild steel in hydrochloric acid. Mater Chem Phys. 2009;113(2):685-9. https://doi.org/10.1016/j.matchemphys.2008.08.028
31. Cao C. On electrochemical techniques for interface inhibitor research. Corros Sci. 1996;38(12):2073-82. https://doi.org/10.1016/S0010-938X(96)00034-0
32. Chafiq M, Chaouiki A, Damej M, et al. Bolaamphiphile-class surfactants as corrosion inhibitor model compounds against acid corrosion of mild steel. J Mol Liq. 2020;309:113070. https://doi.org/10.1016/j.molliq.2020.113070
33. Bashir S, Thakur A, Lgaz H, et al. Computational and experimental studies on Phenylephrine as anti-corrosion substance of mild steel in acidic medium. J Mol Liq. 2019;293:111539. https://doi.org/10.1016/j.molliq.2019.111539
34. Gupta RK, Malviya M, Ansari KR, et al. Functionalized graphene oxide as a new generation corrosion inhibitor for industrial pickling process: DFT and experimental approach. Mater Chem Phys. 2019;236:121727. https://doi.org/10.1016/j.matchemphys.2019.121727
35. Haque J, Srivastava V, Chauhan DS, et al. Electrochemical and surface studies on chemically modified glucose derivatives as environmentally benign corrosion inhibitors. Sustain Chem Pharm. 2020;16:100260. https://doi.org/10.1016/j.scp.2020.100260
36. Goyal M, Kumar S, Verma C, et al. Interfacial adsorption behavior of quaternary phosphonium based ionic liquids on metal-electrolyte interface: Electrochemical, surface characterization and computational approaches. J Mol Liq. 2020;298:111995. https://doi.org/10.1016/j.molliq.2019.111995
37. Singh P, Quraishi M. Corrosion inhibition of mild steel using Novel Bis Schiff's Bases as corrosion inhibitors: Electrochemical and Surface measurement. Measurement. 2016;86:114-24. https://doi.org/10.1016/j.measurement.2016.02.052

38. Li X, Deng S, Xie X. Experimental and theoretical study on corrosion inhibition of o-phenanthroline for aluminum in a HCl solution. J Taiwan Inst Chem Eng. 2014;45(4):1865-75. https://doi.org/10.1016/j.jtice.2013.10.007
39. Amin MA, Ahmed M, Arida H, et al. Monitoring corrosion and corrosion control of iron in HCl by non-ionic surfactants of the TRITON-X series–Part II. Temperature effect, activation energies and thermodynamics of adsorption. Corros Sci. 2011;53(2):540-8. https://doi.org/10.1016/j.corsci.2010.09.019
40. Amin MA, El-Rehim SA, El-Sherbini E, et al. Chemical and electrochemical (AC and DC) studies on the corrosion inhibition of low carbon steel in a 1.0 M HCl solution by succinic acid-temperature effect, activation energies and thermodynamics of adsorption. Int J Electrochem Sci. 2008;3:199-215.
41. Lgaz H, Zehra S, Albayati M, et al. Corrosion Inhibition of Mild Steel in 1.0 M HCl by two Hydrazone Derivatives. Int J Electrochem Sci. 2019;14:6667-81. https://doi.org/10.20964/2019.07.08
42. Chaouiki A, Lgaz H, Salghi R, et al. New Benzohydrazide Derivative as Corrosion Inhibitor for Carbon Steel in a 1.0 M HCl Solution: Electrochemical, DFT and Monte Carlo Simulation Studies. Port Electrochim Acta. 2019;37(3):147-65. https://doi.org/10.4152/pea.201903147
43. Chaouiki A, Lgaz H, Zehra S, et al. Exploring deep insights into the interaction mechanism of a quinazoline derivative with mild steel in HCl: electrochemical, DFT, and molecular dynamic simulation studies. J Adhes Sci Technol. 2019;33(9):921-44. https://doi.org/10.1080/01694243.2018.1554764
44. Bouammali H, Jama C, Bekkouch K, et al. Anticorrosion potential of diethylenetriaminepentakis (methylphosphonic) acid on carbon steel in hydrochloric acid solution. J Ind Eng Chem. 2015;26:270-6. https://doi.org/10.1016/j.jiec.2014.11.039
45. Ansari KR, Quraishi MA, Singh A. Corrosion inhibition of mild steel in hydrochloric acid by some pyridine derivatives: An experimental and quantum chemical study. J Ind Eng Chem. 2015;25:89-98. https://doi.org/10.1016/j.jiec.2014.10.017
46. Khaled K. Molecular simulation, quantum chemical calculations and electrochemical studies for inhibition of mild steel by triazoles. Port Electrochim Acta. 2008;53(9):3484-92. https://doi.org/10.1016/j.electacta.2007.12.030
47. Lgaz H, ELaoufir Y, Ramli Y, et al. Synergistic effect of potassium iodide with (E)-3-(4 methoxystyryl)quinoxalin- 2(1H)-one on the corrosion inhibition of carbon steel in 1.0 M HCl. Pharma Chem. 2015;7(6):36-45.
48. El Aoufir Y, Lgaz H, Bourazmi H, et al. Quinoxaline Derivatives as Corrosion Inhibitors of Carbon Steel in Hydrochloridric Acid Media: Electrochemical, DFT and Monte Carlo simulations studies. J Mater Environ Sci. 2016;7(12):4330-7.
49. Bousskri A, Salghi R, Anejjar A, et al. Pyridazinium-based ionic liquids as corrosion inhibitors for copper in phosphoric acid containing chloride: Electrochemical, surface and quantum chemical comparatives studies. Pharma Chem. 2016;8(2):67-83. https://doi.org/10.4152/pea.201601001

50. Verma C, Quraishi MA, Gupta NK. 2-(4-{[4-Methyl-6-(1-methyl-1H-1,3-benzodiazol-2-yl)-2-propyl-1H-1,3-benzodiazol-1-yl] methyl} phenyl) benzoic acid as green corrosion inhibitor for mild steel in 1 M hydrochloric acid. Ain Shams Eng J 2018;9:1225-1233. https://doi.org/10.1016/j.asej.2016.07.003
51. Verma C, Quraishi MA, Singh A. 2-Amino-5-nitro-4,6-diarylcyclohex-1-ene-1,3,3-tricarbonitriles as new and effective corrosion inhibitors for mild steel in 1 M HCl: Experimental and theoretical studies. J Mol Liq. 2015;212:804-12. https://doi.org/10.1016/j.molliq.2015.10.026
52. Lgaz H, Benali O, Salghi R, et al. Pyridinium derivatives as corrosion inhibitors for mild steel in 1 M HCl: Electrochemical, surface and quantum chemical studies. Der Pharma Chemica. 8th ed. 2016;172-90.
53. Lgaz H, Subrahmanya Bhat K, Salghi R, et al. Insights into corrosion inhibition behavior of three chalcone derivatives for mild steel in hydrochloric acid solution. J Mol Liq. 2017;238:71-83. https://doi.org/10.1016/j.molliq.2017.04.124
54. Lgaz H, Salghi R, Jodeh S, et al. Effect of clozapine on inhibition of mild steel corrosion in 1.0 M HCl medium. J Mol Liq. 2017;225:271-80. https://doi.org/10.1016/j.molliq.2016.11.039